Mechanism of Nitrogen-Concentration Dependence on pH Value: Experimental and Theoretical Studies on Nitrogen-Doped TiO2

ARTICLE *in* THE JOURNAL OF PHYSICAL CHEMISTRY C · AUGUST 2008

Impact Factor: 4.77 · DOI: 10.1021/jp803519q

7 AUTHORS, INCLUDING:

Hongqi Sun
Curtin University
86 PUBLICATIONS **2,049** CITATIONS
SEE PROFILE

Wanqin Jin
California Institute of Technology
224 PUBLICATIONS **4,779** CITATIONS
SEE PROFILE

Guojun Chen
14 PUBLICATIONS **174** CITATIONS
SEE PROFILE

Bingqian Xu
University of Georgia
84 PUBLICATIONS **3,688** CITATIONS
SEE PROFILE

Mechanism of Nitrogen-Concentration Dependence on pH Value: Experimental and Theoretical Studies on Nitrogen-Doped TiO_2

Hongqi Sun,[†] Yuan Bai,[†] Huijing Liu,[†] Wanqin Jin,*[,†] Nanping Xu,[†] Guojun Chen,[‡] and Bingqian Xu[‡]

State Key Laboratory of Materials-Oriented Chemical Engineering, College of Chemistry and Chemical Engineering, Nanjing University of Technology, 5 Xinmofan Road, Nanjing 210009, P. R. China, and Faculty of Engineering & Nanoscale Science and Engineering Center, University of Georgia, Athens, Georgia 30602

Received: April 23, 2008; Revised Manuscript Received: June 14, 2008

Experiments and density functional theory (DFT) calculations were combined in an attempt to investigate the origin of the differences in nitrogen concentration incorporated by N-doped TiO_2. X-ray photoelectron spectroscopy (XPS), UV−vis diffusive reflectance spectra (UV−vis), and photodegradation experiments were conducted to set some premises for DFT calculations. Fourier transform infrared (FT-IR) spectroscopy was applied to investigate the NH_x-containing species in the dried precipitate from the hydrolysis. $[Ti(H_2O)_a(NH_3)_b(OH)_cCl_d]^{(4-c-d)}$ $(a + b + c + d = 6)$ is defined as the Ti complex produced by the hydrolysis process, and its pH-dependent character was further determined by Gibbs energy calculations for the reaction based on those of related equations. Adsorption energies of NO on TiO_2 surfaces were calculated to study the ability of NO_x to be incorporated into the TiO_2 matrix under different pH conditions. Finally, we propose three processes as being responsible for the dependence of the nitrogen concentration on the pH value.

1. Introduction

Recently, many efforts have been directed toward extending the response of TiO_2 to the visible region.[1−5] To obtain a photocatalyst with high activity under both UV and visible-light irradiations, numerous studies have focused on nitrogen-doped TiO_2.[6−10] However, the active species and the mechanism for the visible-light response of N-doped TiO_2 are still open questions. Various chemical states of doped nitrogen such as substitutional N,[6,11−13] NO_x,[7,8,14−16] and NH_x[9] have been proposed as active doping species, which are probably controlled by the preparation conditions.

Our previous studies showed that the properties of ion-doped TiO_2 depend on the method, calcination temperature, and precursor used in the preparation;[17−21] other researchers have also found that the crystal phase, surface characteristics, morphology, particle size, optical properties, and catalytic activity of pure TiO_2 depend on the pH value in the preparation of pure TiO_2.[22−28] However, the effects of pH on nonmetal-ion-doped TiO_2 are still not very well understood.[12,29] Burda et al.[30] mentioned the effect of pH on the doping nitrogen concentration, which would affect the photocatalytic activity of nitrogen-doped TiO_2 directly,[31,32] but their studies did not provide enough evidence on the issue of how the pH value influences the nitrogen doping levels. Therefore, an investigation of the mechanism by which the nitrogen concentration depends on pH would be helpful for the development of new ion-doped TiO_2 photocatalysts.

In this work, we synthesized a series of nitrogen-doped TiO_2 materials controlling the pH value in the $TiCl_4$ hydrolysis processes. We suggest that the nitrogen concentration in N−TiO_2 mainly relies on the two processes of hydrolysis and calcination. With combined analysis of surface characterizations and photodegradation experiments, calculations using density functional theory (DFT) were also performed to simulate the processes of hydrolysis[33] and calcination[34] from the perspective of coordination chemistry[35] and surface chemistry,[26] respectively. Then, a mechanism for the effect of pH on the nitrogen concentration is proposed based on the results of experiments and DFT calculations.

2. Experimental Details

2.1. Preparation. Each nitrogen-doped TiO_2 sample (photocatalyst) was prepared following our reported procedure.[20] The pH value of the $TiCl_4$ solution was adjusted to 3.5, 5.5, 7.5, and 9.5 using 3 M NaOH or HCl aqueous solution, and the as-prepared nitrogen-doped TiO_2 samples are denoted as TN3.5, TN5.5, TN7.5, and TN9.5, respectively.

Acid washing experiments were performed as follows: A 0.50-g sample of powder was added to 50 mL of water with three drops of concentrated HCl (12 mol L^{-1}), and the suspension was ultrasonically dispersed for 15 min and stirred for 4 h. Then, the powder was collected by high-speed centrifugation, washed several times with water, and dried at 353 K under reduced pressure to remove the water in the powder.

2.2. Characterization. The states of the charges were investigated by X-ray photoelectron spectroscopy (XPS) using an ESCALab MK2 instrument with a Mg X-ray source. UV−vis reflectance spectra were measured with a Shimadzu UV-2401TC UV−vis spectrophotometer, using $BaSO_4$ as the background. The concentration of 4-chlorophenol (4-CP) was determined by measuring the decrease of the absorbance at 225 nm on a Perkin-Elmer Lambda 35 UV−vis spectrophotometer. Fourier transform infrared (FT-IR) spectroscopy was performed on a Thermo Nicolet Avatar-360 spectrometer in the range of 4000−400 cm^{-1} by the KBr pellet method.

* Corresponding author. Tel.:+86-25-83587211. Fax: +86-25-8358-7211. E-mail: wqjin@njut.edu.cn.
[†] Nanjing University of Technology.
[‡] University of Georgia.

10.1021/jp803519q CCC: $40.75
Published on Web 08/06/2008

2.3. Evaluation of the Photocatalytic Activity. The photocatalytic activities in the photodegradation of 4-chlorophenol were evaluated for both the bare and acid-washed samples by measuring the apparent reaction rate constants. Detailed information on these measurements can be found in the literature.[20]

3. Computational Details

Reaction free energies were obtained by performing electronic structure calculations on the reactants and products in the proposed equations.[33,35] These calculations employed the DFT software package DMol3.[36] The geometry optimizations were carried out and the free energies were obtained at the generalized gradient approximation (GGA) level. The exchange-correlation energy was approximated by BLYP with double numerical plus polarization (DNP) basis sets.[37,38] The self-consistent field (SCF) convergence was set to 10^{-6}, and the convergence criterion for the gradient in geometry optimizations was set to 10^{-3} hartree per bohr. Vibration frequencies for each reactant and product were obtained from a normal-mode analysis of the calculated Hessian matrix, from which translational and rotational degrees of freedom were projected. Then, molecular free energies were obtained by calculation of the temperature-dependent partition functions needed in the statistical mechanical expression. The ΔG(g) value derived from ΔG(DFT) was changed to ΔG(aq) using the correlations provided in the literature.[33]

The most stable (001) surface has been widely used to represent TiO_2 crystal surface,[26,33,34,39] so it was selected as the typical crystal surface of anatase TiO_2 in the calculations. NO was selected to be the model of NO_x because it not only is produced in oxidation of NH_4Cl but also is present in most NO_x-doped TiO_2 photocatalysts.[8,20,21,31] A (2 × 2) (001) stoichiometric anatase surface structure with a 10-Å vacuum layer was used in the calculations, and dissociatively adsorbed water partially covered the face,[40] with H and OH terminations oriented perpendicular to the surface to represent acidic, neutral, and alkaline conditions.[26,41] These calculations were performed with the DFT software package CASTEP.[36] Optimized geometries and adsorption energies of NO on the TiO_2 surface were calculated using DFT within the GGA, with the exchange-correlation functional of Perdew and Wang (PW91).[42] The energy cutoff was set to 300.0 eV, and a 4 × 4 × 4 Monkhorst−Pack k point was employed for both the initial relaxations of the structures and the final calculations of surface energies.

4. Results and Discussion

Based on an analysis of XRD and nitrogen adsorption−desorption isotherms (which can be found in Supporting Information), it was found that the as-prepared samples were all dominantly of the anatase phase, with little brookite phase, and had a mesoporous structure. With increasing pH, the anatase phase content, intensities of the (101) peaks, and average crystallite size (9.5, 10.6, 12.7, and 20.7 nm for TN3.5, TN5.5, TN7.5, and TN9.5, respectively) of the samples increased, but the specific surface areas of the samples decreased (99.0, 96.6, 90.1, and 78.7 m^2/g for TN3.5, TN5.5, TN7.5, and TN9.5, respectively). In low-pH conditions, the quantity of hydroxyl groups in hydrolysis is small, which prevents the crystallization of the samples and the growth of the TiO_2 crystallites. With increasing pH, more hydroxyl groups are available for the hydrolysis, which leads to better crystallization of TiO_2 and greater crystallite sizes. The fact that the BET specific surface areas decreased with increasing pH value might be due to the increase in the crystallite size or the increase in the pore size of the TiO_2 powders.[28,29]

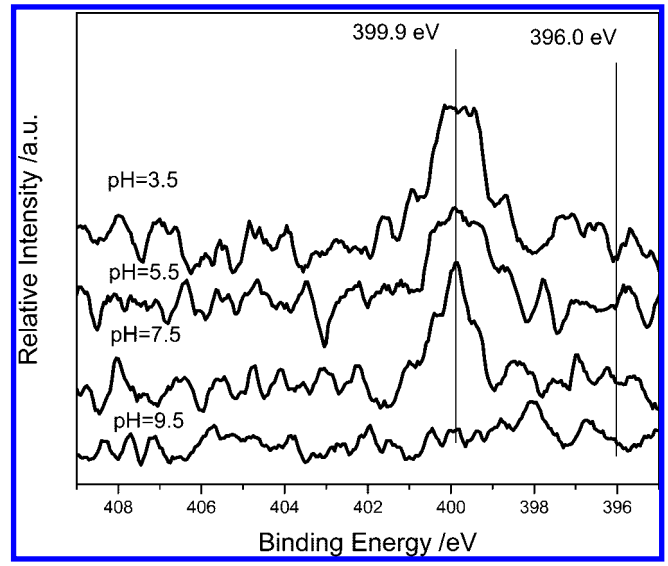

Figure 1. N 1s XPS spectra of the nitrogen-doped TiO_2 obtained at various pH values.

4.1. XPS Studies. Figure 1 shows N 1s XPS spectra for the doped samples in which all peaks were calibrated with respect to the C 1s peak at 284.8 eV. The nitrogen concentrations in samples TN3.5, TN5.5, TN7.5, and TN9.5 were calculated as 0.49%, 0.28%, 0.36%, and 0.05%, respectively. Strong peaks centered at 399.9 eV were found in the samples of TN3.5, TN5.5, and TN7.5. With increasing pH value, the peak at 399.9 eV became sharper, eventually disappearing at pH 9.5. It is well-known that the XPS signal at around 400 eV is the subject of controversy in the identification of nitrogen species in the field of nitrogen-doping materials. Most studies concerned with substitutional N doping[6,11−13,32] have attributed this peak (400 eV) to molecularly chemisorbed γ-N_2, which is not responsible for the visible response of N−TiO_2, even though this signal is usually stronger than that at 396 eV in most of the investigated samples.[6,11−13,32] However, many studies have suggested that the signal at 400 eV is also critical for a visible-light response, because the signal at 396 eV is completely absent from so-called NO_x-doped TiO_2.[7,8,14−16,31] Even in the field of NO_x doping, the identification of the XPS signal at about 400 eV still attracts much dissension. Sathish et al.[14] suggested that the N 1s peak at 398.2 eV should be attributed to the anionic N^- in O—Ti—N linkages and that the nitrogen from NO or NO_2 should appear above 400 eV. Kisch et al.[15] assigned the signal at 400.1 eV to the presence of hyponitrite. Sato et al.[16] pointed out that the assignment of the N 1s peak at 400 eV to chemisorbed molecular N_2 is implausible, because N_2 is not chemisorbed on TiO_2 at room temperature, and they concluded that the N 1s peak at 400 eV originates from an oxidized state similar to NO species. The excellent studies carried out by Burda et al.[8,30,31] also showed that the N 1s signal at 400 eV should be NO, based on experiments and the observations of previous studies. XPS and electron paramagnetic resonance (EPR) techniques as well as DFT calculations were combined by Giamello et al.[43−45] to characterize the active species of nitrogen-doped TiO_2, and the results indicated that there are two types of paramagnetic species in the bulk of nitrogen-doped TiO_2. It is recalled that our nitrogen-doped TiO_2 samples has a mesoporous structure; therefore, it is possible that a series of NO_x species could exist in the surface structure.[20,21] The direct evidence for confirming that the N 1s peak at about 400 eV

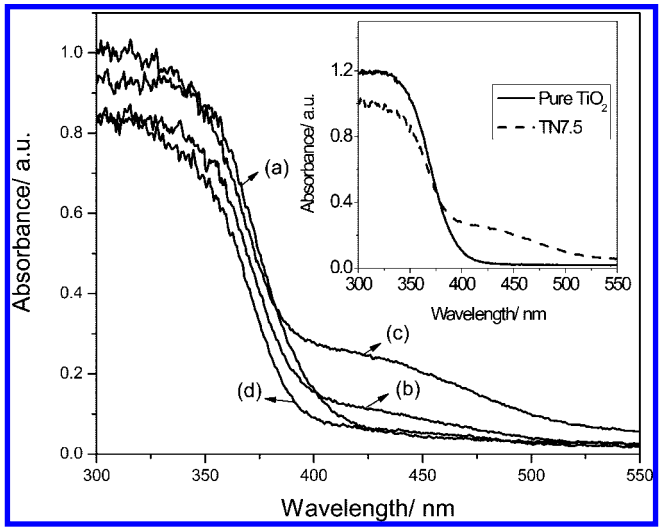

Figure 2. UV−vis spectra of various samples: (a) TN3.5, (b) TN5.5, (c) TN7.5, (d) TN9.5. Inset: Comparison between pure and nitrogen-doped TiO_2.

should be NO was reported by DeLouise et al.[46] and Rodriguez et al.[47] They both observed that the XPS signal of N 1s at about 400 eV appears when NO is adsorbed on a crystallite surface.[46,47] For the reasons mentioned above, the N 1s peak at 399.9 eV in this work was attributed to NO species. With increasing pH, the peak at 399.9 became sharper, and its intensity decreased, indicating that both the total doping level and the relative amount of NO species in TiO_2 are affected by the pH value. The weak peaks in the region of 396−398 eV, which probably arise from O−Ti−N linkages,[14] increase with decreasing pH.

4.2. UV−Vis Diffuse Absorption Spectra. UV−vis spectra of pure and doped TiO_2 are displayed in Figure 2, which shows that the response of the nitrogen-doped TiO_2 is extended to the visible region. A significant decrease at wavelengths shorter than 400 nm can be attributed to the excitation of electrons from the valence band to the conduction band of TiO_2, and the band gap of pure TiO_2 is estimated to be 3.16 eV. Compared with the pure TiO_2 sample, the band-gap energies of the doped samples shift to lower energy, with values 3.08, 3.12, 3.13, and 3.15 eV being found for TN3.5, TN5.5, TN7.5, and TN9.5, respectively. Minor band-gap narrowing can be ascribed to the presence of trace amounts of anionic nitrogen atoms N^{3-} or N^- in the matrix of TiO_2,[6,14] which is consistent with the XPS results. The new absorption bands (from 400 to 550 nm) of the doped samples might arise from surface states or impurity energy bands.[8,14−16] The absorption intensities of the doped samples in the visible region follow the order TN7.5 > TN5.5 > TN3.5 > TN9.5, which can also be seen in Figure 2. This result is in agreement with the finding on the trend in the intensity of the N 1s XPS signals at 399.9 eV, which was assigned to NO.

4.3. Photocatalytic Activity. Generally, the photodegradation reaction of 4-CP can be described by the Langmuir−Hinshelwood mechanism, and the photocatalytic activity of the catalysts can be quantitatively evaluated with the equation

$$\ln \frac{C}{C_0} = kt \qquad (1)$$

where k is the apparent reaction rate constant and C_0 and C represent the concentrations of 4-CP at the initial time and time t, respectively.[17,20] As shown in Figure 3A, the activities of all doped samples except TN9.5 are higher than that of pure TiO_2 under UV irradiation. With increasing pH, the activity first

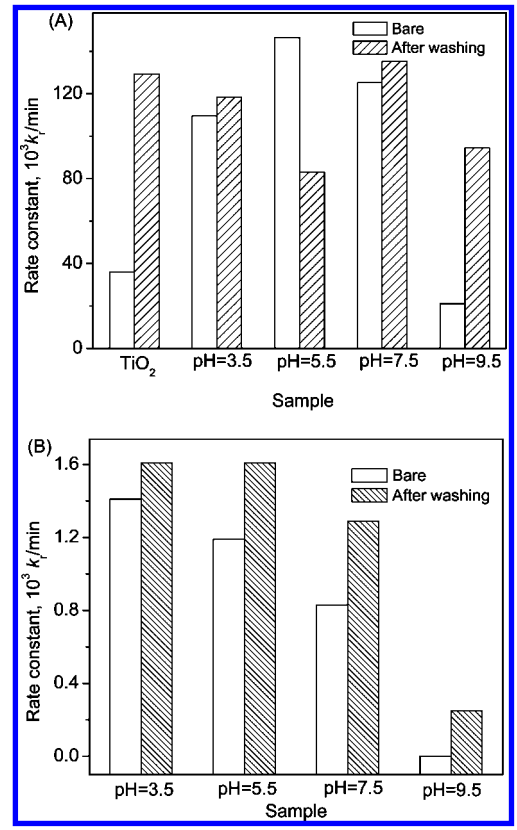

Figure 3. Dependence of the apparent reaction rate constant of the samples on pH: (A) under UV irradiation, (B) under visible-light irradiation.

increases and then decreases, and sample TN5.5 exhibits the highest activity among the as-synthesized photocatalysts. After acid washing, the activity of TN5.5 decreases, and the activities of the other samples (including pure TiO_2) increase. The difference in activity before and after acid washing is highest for sample TN9.5 among that of the as-prepared samples. Figure 3B shows the efficiencies of the doped samples under visible irradiation. With increasing pH, the activity of the catalyst decreases, ultimately becoming very low at pH 9.5; moreover, the differences in activity between the bare and acid-washed samples become larger.

The results of the photodegradation of 4-CP clearly reveal that acid washing of N−TiO_2 strongly influences its activity; such a phenomenon also was observed by Kisch et al.[15] Fu et al.[48] demonstrated that absorbed NH_3 can be removed by washing with pure water, and they also observed that doping species might be oxidized during reactions. Moreover, the chemical states and nitrogen concentration were found to vary with the profile of TiO_2 using Ar^+ sputtering by Viswanath et al.;[49] similar results were reported in our previous work.[17] Combining our results in this work with the reports of other researechers, we can conclude that the interactions between impurities and the TiO_2 surface play a key role in determining the characteristics of nitrogen-doped TiO_2.

Analysis of all of the experiments mentioned above provided some primary bases for investigating the nature of the nitrogen-concetration dependence on pH: (a) The nitrogen concentration depends strongly on the pH value; (b) the chemical states of impurities, which are related to the concentration of NO or anionic nitrgoen atoms, vary with pH; and (c) strong interactions exist between NO_x and the TiO_2 surface. Thus, we carried out an investigation from hydrolysis to calcination as described in the following sections.

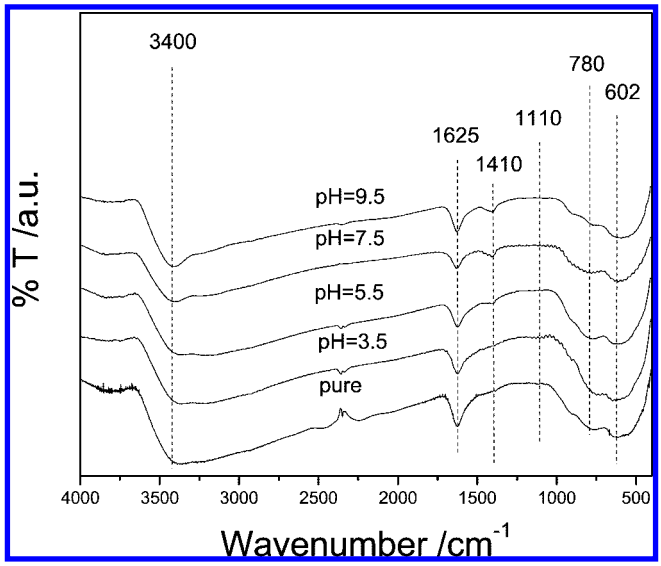

Figure 4. FT-IR spectra of dried gelatins of pure TiO_2 and nitrogen-doped TiO_2 obtained at various pH values.

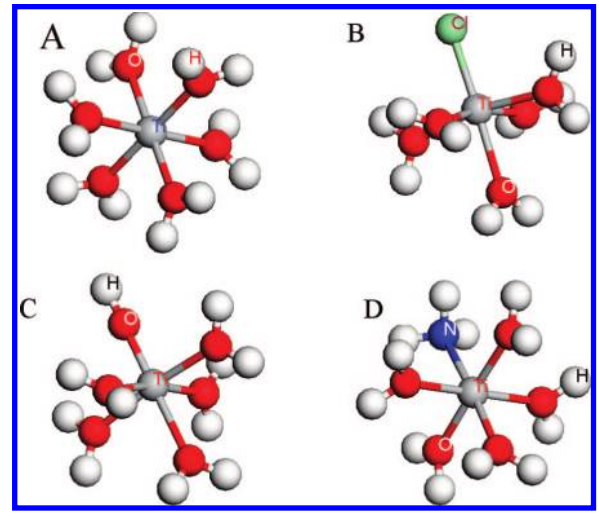

Figure 5. Molecular structures of various Ti complexes: (A) $[Ti(H_2O)_6]^{4+}$, (B) $[Ti(H_2O)_5Cl]^{3+}$, (C) $[Ti(H_2O)_5OH]^{3+}$, (D) $[Ti(H_2O)_5NH_3]^{4+}$.

4.4. Hydrolysis of $TiCl_4$ with Addition of N Precursors. The process of $TiCl_4$ hydrolysis has been investigated widely for the preparation of nanosize TiO_2. It involves a complicated L−S (liquid−solid) system containing H_2O, Ti^{4+}, H^+, Cl^-, OH^-, $Ti(OH)_4$, $TiOCl_2$, etc. The concept of coordination chemistry has been used to describe the complex $[Ti(OH)_nCl_m]^{2-}$ in several studies.[27,35,50] To obtain an overview of the hydrolysis of $TiCl_4$ with N precursors, a modified term of the form $[Ti(H_2O)_a(NH_3)_b(OH)_cCl_d]^{(4-c-d)}$ (where $a + b + c + d = 6$ and N_2H_4 was neglected because of its similarity to NH_3) was used in this work. Then, the precipitate from hydrolysis could include two types of N-containing compounds: NH_4Cl and NH_3 in Ti complexes.

4.4.1. NH_4Cl Incorporated in the Precipitate. Previously, we constructed a combined method to investigate the nonmetal-ion doping process using FT-IR spectroscopy and the combination of thermogravimetry and differential scanning calorimetry (TG-DSC).[17] FT-IR spectra were also used in this work to characterize the powder of dried precipitate, as shown in Figure 4. Two peaks at 3400 and 1625 cm^{-1} are assigned to the adsorbed water and hydroxyl of the samples; the peak at 3400 cm^{-1} also covers the N—H vibration, and the other two bands at 602 and 780 cm^{-1} arise from Ti—O stretches of amorphous TiO_2.[51] The band at 1410 cm^{-1} can be attributed to the bending vibration of NH_4^+.[10,52] The peak at 1410 cm^{-1} is not found in pure TiO_2, and it increases with increasing pH for doped samples, probably indicating that more NH_4Cl is incorporated at higher pH. Greater incorporation of NH_4Cl can be ascribed to the rapid precipitation process, which is promoted by increasing OH^- concentration. Recall that the N doping level decreases with increasing pH, which is contrary to the dependence of the amount of NH_4Cl on the pH, indicating the incorporation of NH_4Cl in the precipitate is not the key step in determining the N-doping concentration. A very weak signal at 1110 cm^{-1} was found for the samples obtained at pH 3.5 and 5.5. Kisch et al.[15] assigned this signal to hyponitrite, Ihara et al.[10] suggested that the peak at 1171 cm^{-1} can be assigned to NH_3, and Dai et al.[53] assigned the peak at 1090 cm^{-1} to nitrogen atoms embedded in TiO_2. Because the samples were not subjected to calcination, we propose that this peak can be assigned to NH_3 in the complex $[Ti(H_2O)_a(NH_3)_b(OH)_cCl_d]^{(4-c-d)}$ (where $a + b + c + d = 6$). The amount of NH_4Cl in the powders before calcination showed roughly an inverse relationship to the nitrogen concentration of the resulting nitrogen-doped TiO_2, so the NH_3 in the Ti complex possibly contributes to the enhancement of the nitrogen concentration at low pH.

4.4.2. NH_3 in the Ti Complex. Because no thermodynamic data are available for $[Ti(H_2O)_a(NH_3)_b(OH)_cCl_d]^{(4-c-d)}$ ($a + b + c + d = 6$), DFT calculations were carried out to investigate the NH_3-containing complex.[33] The molecular models of the complexes are shown in Figure 5, and the possible coordination reactions are listed in eqs 2−6, where the reactants have been simplified.

$$[Ti(H_2O)_6]^{4+}(g) + NH_3(g) = [Ti(H_2O)_5NH_3]^{4+}(g) + H_2O(g) \quad (2)$$

$$[Ti(H_2O)_6]^{4+}(g) + Cl^-(g) = [Ti(H_2O)_5Cl]^{3+}(g) + H_2O(g) \quad (3)$$

$$[Ti(H_2O)_6]^{4+}(g) + OH^-(g) = [Ti(H_2O)_5OH]^{3+}(g) + H_2O(g) \quad (4)$$

$$[Ti(H_2O)_5NH_3]^{4+}(g) + OH^-(g) = [Ti(H_2O)_5OH]^{3+}(g) + NH_3(g) \quad (5)$$

$$[Ti(H_2O)_5OH]^{3+}(g) + H^+(g) + NH_3(g) = [Ti(H_2O)_5NH_3]^{4+}(g) + H_2O(g) \quad (6)$$

The calculated thermodynamic parameters for the reactants in eqs 2−6 are summarized in Table 1. To maintain coherence, $\Delta G(g)$ values for eqs 2−6 were calculated using the data from DFT results, which were determined to be 0.275, −2.513, 5.294, 5.019, and 10.105 kcal mol^{-1}, respectively. The corresponding liquid-phase reaction energies [G(aq)] deduced from eq 7[33] were calculated as −10.141,−12.754,−5.437,−5.694, and −0.928 kcal mol^{-1}, respectively.

$$\Delta G(DFT) = 1.067[\Delta G(aq)] + 11.095 \quad (7)$$

Equations 2−4 were used to investigate the formation of $[Ti(H_2O)_5NH_3]^{4+}$, $[Ti(H_2O)_5Cl]^{3+}$, and $[Ti(H_2O)_5OH]^{3+}$. Each G(aq) value for these equations was negative, indicating the formation of the three Ti complexes in the hydrolysis process. Equations 5 and 6 can represent the variety of NH_3-containing

TABLE 1: Thermodynamic Parameters of the Investigated Processes

material	$\Delta H_{298.15}^{\circ}$ (kcal/mol)	$\Delta S_{298.15}^{\circ}$ [cal/(mol K)]	$\Delta G_{298.15}^{\circ}$ (kcal/mol)
$H^+(g)$	1.333	30.6825	−7.815
$OH^-(g)$	6.591	41.299	−5.722
$Cl^-(g)$	1.333	41.232	−10.96
$NH_3(g)$	23.696	48.156	9.339
$H_2O(g)$	15.395	46.749	1.537
$[Ti(H_2O)_6]^{4+}(g)$	101.924	107.788	69.787
$[Ti(H_2O)_5NH_3]^{4+}(g)$	110.421	109.197	77.864
$[Ti(H_2O)_5Cl]^{3+}(g)$	87.748	110.586	54.777
$[Ti(H_2O)_5OH]^{3+}(g)$	102.437	116.267	67.772

Ti complexes at different pH values. The values of G(aq) for eqs 5 and 6 suggest that the amount of $[Ti(H_2O)_5NH_3]^{4+}$ species decreases with increasing pH; that is, higher pH should promote the hydrolysis process and decrease the amount of $[Ti(H_2O)_5NH_3]^{4+}$, which might be adsorbed or encapsulated during the precipitation of $Ti(OH)_4$. The results are consistent with the observations of Burda et al.[30]

From the above analysis, a schematic graph can be developed to explain the evolution with pH of the species involved in the solution, as shown in Figure 6. The values of a, b, and d in $[Ti(H_2O)_a(NH_3)_b(OH)_cCl_d]^{(4-c-d)}$ $(a + b + c + d = 6)$ decrease with increasing pH, whereas c and the amount of NH_4Cl increase in this process. It is concluded that the doping nitrogen might derive from two types of N-containing compositions incorporated by the precipitation: NH_4Cl and NH_3 in the Ti complex. NH_4Cl would be located at longer distances from the Ti atoms, whereas NH_3 in the Ti complex would be closer to the Ti atoms. Our previous studies[17] demonstrated that the distribution of precursors plays an important role in ion-doping process, with shorter distances between the ion donor and the Ti precursor leading to easier doping processes. In the present work, the distance between the N of NH_4Cl in the precipitate and the Ti precursor is greater than that of the N in the NH_3 in the Ti complex; thus, the amount of NH_3 in the Ti complex probably plays the most important role in determining the doping nitrogen concentration. This is plausible because NH_3 in the Ti complex would be decomposed during the crystal transformation process, which might make nitrogen atoms easier to incorporate into the TiO_2 matrix.[17,30] We did not evaluate the impact factor quantitively because of the difficulty of obtaining the formation constant of $[Ti(H_2O)_a(NH_3)_b(OH)_cCl_d]^{(4-c-d)}$ $(a + b + c + d = 6)$. DSC measurements did not show any difference in the exothermic peak for the decomposition of NH_4Cl and NH_3 in the Ti complex because of their low concentrations. However, the TG curves showed an increasing weight loss with increasing pH, indicating an increased hydroxyl content in the powder at higher pH values.

4.5. Interaction of Calcination Products with the TiO_2 Surface. As indicated by the XPS and UV−vis observations, most of the doping species were NO. Furthermore, photocatalysis of the acid-washed samples showed that most of the nitrogen species were located on the surface of the TiO_2. With this evidence, we propose that a key factor in determining the nitrogen concentration is the adsorption property of NO on the TiO_2 surface. A higher doping nitrogen concentration can probably be attributed to a larger adsorption energy. To investigate the adsorption properties of NO on the TiO_2 surface at various pH values, the adsorption energies were calculated using the DFT method.

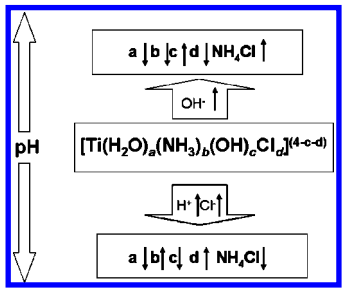

Figure 6. Schematic graph of the evolution of species with pH value.

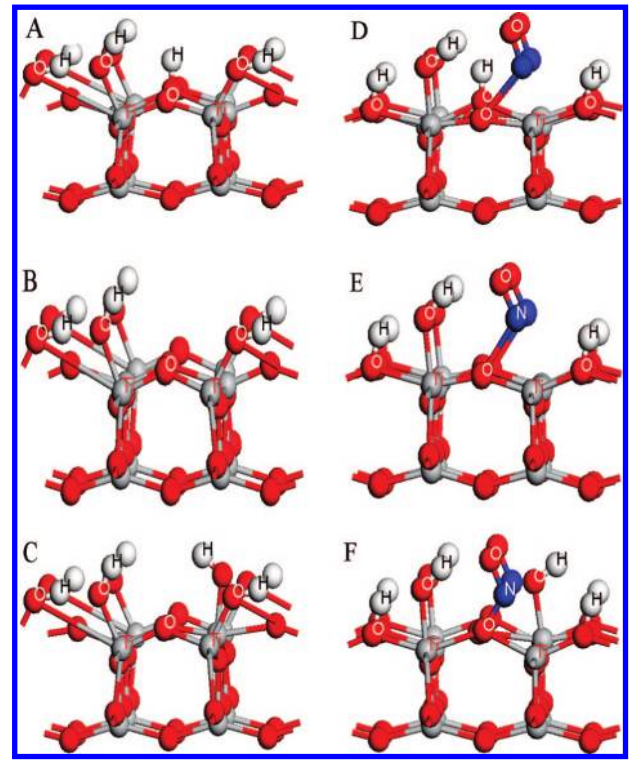

Figure 7. Surface structures of the modified TiO_2(001) surfaces: (A) Suf_{T-H}, (B) Suf_{T-W}, (C) Suf_{T-OH}, (D) Suf_{T-H-N}, (E) Suf_{T-W-N}, (F) Suf_{T-OH-N}.

The stoichiometric (001) surface was selected as a typical crystal surface of anatase TiO_2 because it is active for catalysis and will appear upon calcination.[26,33,34,39] Then, a constant (2 × 2) (001) surface that was partially covered by water was constructed[40] and is denoted as Suf_{T-W}. The TiO_2 surfaces obtained at acidic, neutral, and alkaline conditions were constructed as suggested by Barnard et al.[26,40,41] and are denoted as Suf_{T-H}, Suf_{T-W}, and Suf_{T-OH}, respectively. The final surfaces of nitrogen-doped TiO_2 were constructed as NO adsorbed on the surface of pure TiO_2 and TiO_2 with H and OH groups and are denoted as Suf_{T-H-N}, Suf_{T-W-N}, and Suf_{T-OH-N}, respectively. All of these surface models are shown in Figure 7. The geometries of the surface structures were optimized, and the total energies were calculated. The methodology was tested by calculating the cell parameters of bulk anatase TiO_2, $a = b =$ 3.797 Å and $c = 9.775$ Å, and comparing the results to the experimental data, $a = b = 3.78$ Å and $c = 9.514$ Å. The total energies for each structure and NO molecular are listed in Table 2. The adsorption energies were calculated as[34]

$$E_{ads} = E_{surface} + E_{adsorbate} - E_{model} \quad (8)$$

where $E_{surface}$ is the energy of the reference surface, $E_{adsorbate}$ is the energy of NO, and E_{model} is the energy of the nitrogen-doped TiO_2 surface. The adsorption energies of the TiO_2 surface obtained at acidic, neutral, and alkaline conditions were calculated as 1.4246, 0.4333, and 1.7325 eV, respectively, and

TABLE 2: Total Energies of Various Surface Structures and NO Molecule

structure	total energy (eV)
NO molecule	−706.4330
Suf_{T-H}	−20385.9732
Suf_{T-W}	−20370.1663
Suf_{T-OH}	−20823.0822
Suf_{T-H-N}	−21093.8308
Suf_{T-W-N}	−21077.0326
Suf_{T-OH-N}	−21531.2477

these results suggest that the ability to incorporate NO on TiO_2 follows the trend alkaline > acidic > neutral conditions. This trend should be parallel to that of the doped nitrogen concentrations, although it is not agreement with the XPS observations, because the adsorption conditions under consideration were not identical. In other words, different amounts of NO are available to be adsorbed or doped depending on the different amounts of NH_4Cl and NH_3 when the adsorption or doping process occurs.[17] This result suggests that calcination is not the most important step in determining the N-doping levels.

5. Conclusion

A series of visible-light-driven nitrogen-doped TiO_2 were synthesized by the hydrolysis of $TiCl_4$ with addition of nitrogen precursors at various pH values. XPS showed that most of the impurities were NO, as well as trace amounts of nitrogen atoms in O—Ti—N linkages. The activities in the photodegradation of 4-chlorophenol for all of the samples were evaluated under both ultraviolet (UV) and visible-light irradiation. The process of acid washing the TiO_2 has a significant effect, resulting in most of the NO_x locating on the surface of TiO_2. Density functional theory (DFT) was further applied to theoretically model the nature of the nitrogen-concentration dependence on the pH value. Three processes were thought to be responsible for the effect of pH on the nitrogen concentration, such as the adsorption or encapsulation of NH_4Cl in the precipitate, the formation of NH_3 in the Ti complex, and the adsorption relationship between NO_x and the TiO_2 surface. Eventually, on the basis of experimental results combined with DFT calculations, we propose that the formation of NH_3 in the Ti complex plays the most important role in determining the nitrogen concentration in nitrogen-doped TiO_2.

Acknowledgment. DFT calculations were supported by the Department of Materials & Engineering, Nanjing University. We thank Prof. Xiaoming Ren (College of Sciences, Nanjing University of Technology) for his constructive suggestions. This work was sponsored by Program for Changjiang Scholars and Innovative Research Team in University (No. IRT0732), the National High Technology Research and Development Program (2006AA030204), the National Natural Science Foundation (20636020), and the Natural Science Foundation of Jiangsu Province (BK2006722) of China.

Supporting Information Available: XRD, nitrogen adsorption−desorption isotherms, TG-DSC. This material is available free of charge via the Internet at http://pubs.acs.org.

References and Notes

(1) Hoffmann, M. R.; Martin, S. T.; Choi, W.; Bahemann, D. W. *Chem. Rev.* **1995**, *95*, 69.
(2) Anpo, M.; Takeuchi, M. *J. Catal.* **2003**, *216*, 505.
(3) Li, X. Z.; Li, F. B.; Yang, C. L.; Ge, W. K. *J. Photochem. Photobiol. A* **2001**, *141*, 209.
(4) Mor, G. K.; Shankar, K.; Paulose, M.; Varghese, O. K.; Grimes, C. A. *Nano Lett.* **2006**, *6*, 215.
(5) Khan, S. U. M.; Al-Shahry, M.; Ingler, W. B., Jr. *Science* **2002**, *297*, 2243.
(6) Asahi, R.; Morikawa, T.; Ohwaki, T.; Aoki, K.; Taga, Y. *Science* **2001**, *293*, 269.
(7) Sato, S. *Chem. Phys. Lett.* **1986**, *123*, 126.
(8) Chen, X.; Lou, Y.; Samia, A. C. S.; Burda, C.; Gole, J. L. *Adv. Funct. Mater.* **2005**, *15*, 41.
(9) Diwald, O.; Thompson, T. L.; Zubkov, T; Goralski, E. G.; Walck, S. D.; Yates, J. T., Jr. *J.Phys.Chem.B* **2004**, *108*, 6004.
(10) Ihara, T.; Miyoshi, M.; Iriyama, Y.; Matsumoto, O.; Sugihara, S. *Appl. Catal. B* **2003**, *42*, 403.
(11) Morikawa, T.; Asahi, R.; Ohwaki, T.; Aoki, K.; Taga, Y. *Jpn. J. Appl. Phys.* **2001**, *40*, L 561.
(12) Yin, S.; Aita, Y.; Komatsu, M.; Wang, J.; Tang, Q.; Sato, T. *J. Mater. Chem.* **2005**, *15*, 674.
(13) Hong, Y. C.; Bang, C. U.; Shin, D. H.; Uhm, H. S. *Chem. Phys. Lett.* **2005**, *413*, 454.
(14) Sathish, M.; Viswannathan, B.; Viswanath, R. P.; Gopinath, C. S. *Chem. Mater.* **2005**, *17*, 6349.
(15) Sakthivel, S.; Janczarek, M.; Kisch, H. *J. Phys. Chem. B* **2004**, *108*, 19384.
(16) Sato, S.; Nakamura, R.; Abe, S. *Appl. Catal. A* **2005**, *284*, 131.
(17) Sun, H.; Bai, Y.; Cheng, Y.; Jin, W.; Xu, N. *Ind. Eng. Chem. Res.* **2006**, *45*, 4971.
(18) Cheng, Y.; Sun, H.; Jin, W.; Xu, N. *Chem. Eng. J.* **2007**, *128*, 127.
(19) Cheng, Y.; Sun, H.; Jin, W.; Xu, N. *Chin. J. Chem. Eng.* **2007**, *15*, 178.
(20) Sun, H.; Bai, Y.; Cheng, Y.; Jin, W.; Xu, N. *Solar Energy Mater. Solar Cells* **2008**, *92*, 76.
(21) Sun, H.; Bai, Y.; Cheng, Y.; Jin, W.; Xu, N., in revision.
(22) Sugimoto, T.; Okada, K.; Itoh, H. *J. Colloid Interface Sci.* **1997**, *193*, 140.
(23) Neppolian, B.; Yamashita, H.; Okada, Y.; Nishijima, H.; Anpo, M. *Catal. Lett.* **2005**, *105*, 111.
(24) Peng, T.; Song, H.; Xiao, J.; Liu, H.; Qin, J. *J. Non-Cryst. Solids* **2006**, *352*, 3167.
(25) Yu, Y.; Xu, D. *Appl. Catal. B* **2007**, *73*, 166.
(26) Barnard, A. S.; Curtiss, L. A. *Nano Lett.* **2005**, *5*, 1261.
(27) Pottier, A.; Cassaignon, S.; Chaneac, C.; Villain, F.; Tronc, E.; Jolivet, J. P. *J. Mater. Chem.* **2003**, *13*, 877.
(28) Yu, J.; Su, Y.; Cheng, B.; Zhou, M. *J. Mol. Catal. A* **2006**, *258*, 104.
(29) Yin, S.; Aita, Y.; Komatsu, M.; Sato, T. *J. Eur. Ceram. Soc.* **2006**, *26*, 2735.
(30) Qiu, X.; Zhao, Y.; Burda, C. *Adv. Mater.* **2007**, *19*, 3995.
(31) Burda, C.; Lou, Y.; Chen, X.; Samia, A. C. S.; Stout, J.; Gole, J. L. *Nano Lett.* **2003**, *3*, 1049.
(32) Irie, H.; Watanabe, Y.; Hashimoto, K. *J. Phys. Chem. B* **2003**, *107*, 5483.
(33) Hancock, R. D.; Bartolotti, L. *J. Inorg. Chem.* **2005**, *44*, 7175.
(34) Mguig, B.; Calatayud, M.; Minot, C. *Surf. Rev. Lett.* **2003**, *10*, 175.
(35) Cheng, H.; Ma, J.; Zhao, Z.; Qi, L. *Chem. Mater.* **1995**, *7*, 663.
(36) Dmol3 and CASTEP. are available from Accelrys, San Diego, CA.
(37) Lee, C.; Yang, W.; Parr, R. G. *Phys. Rev. B* **1988**, *37*, 785.
(38) Becke, A. D. *J. Chem. Phys.* **1988**, *88*, 2547.
(39) Diebold, U, *Surf. Sci. Rep.* **2003**, *48*, 53, and references therein.
(40) Barnard, A. S.; Zapol, P.; Curtiss, L. A. *J. Chem. Theory Comput.* **2005**, *1*, 107.
(41) Barnard, A. S.; Zapol, P.; Curtiss, L. A. *Surf. Sci.* **2005**, *582*, 173.
(42) Pewdew, J. P.; Wang, Y. *Phys. Rev. B* **1992**, *45*, 13244.
(43) Valentin, C. D.; Pacchioni, G.; Selloni, A.; Livraghi, S.; Giamello, E. *J. Phys. Chem. B* **2005**, *109*, 11414.
(44) Livraghi, S.; Votta, A.; Paganini, M. C.; Giamello, E. *Chem. Commun.* **2005**, *498*.
(45) Livraghi, S.; Paganini, M. C.; Giamello, E.; Selloni, A.; Valentin, C. D.; Pacchioni, G. *J. Am. Chem. Soc.* **2006**, *126*, 15666.
(46) DeLouise, L. A.; Winogard, N. *Surf. Sci.* **1985**, *159*, 199.
(47) Jirsak, T.; Dvorak, J.; Rodriguez, J. A. *Surf. Sci.* **1999**, *436*, L683.
(48) Chen, X.; Wang, X.; Hou, Y.; Huang, J.; Wu, L.; Fu, X. *J. Catal.* **2008**, *255*, 59.
(49) Sathish, M.; Viswanathan, B.; Viswanath, R. P. *Appl. Catal. B* **2007**, *74*, 307.
(50) Chen, Y.; Lin, A.; Gan, F. *Powder Technol.* **2006**, *167*, 109.
(51) Peng, F.; Cai, L.; Yu, H.; Wang, H.; Yang, J. *J. Solid State Chem.* **2008**, *181*, 130.
(52) Mozia, S.; Tomaszewska, M.; Kosowska, B.; Grzmil, B.; Morawski, A. W.; Kalucki, K. *Appl. Catal. B* **2005**, *55*, 195.
(53) Xu, J.; Dai, W.; Li, J.; Cao, Y.; Li, H.; He, H.; Fan, K. *Catal. Commun.* **2008**, *9*, 146.

JP803519Q